Spatiotemporal distribution of heparan sulfate epitopes during myogenesis and synaptogenesis: A study in developing mouse intercostal muscle

ARTICLE *in* DEVELOPMENTAL DYNAMICS · SEPTEMBER 2002

Impact Factor: 2.38 · DOI: 10.1002/dvdy.10138 · Source: PubMed

4 AUTHORS, INCLUDING:

Theo Hafmans
Radboud University Nijmegen
64 PUBLICATIONS **1,710** CITATIONS

SEE PROFILE

DEVELOPMENTAL DYNAMICS 225:70–79 (2002)

Spatiotemporal Distribution of Heparan Sulfate Epitopes During Myogenesis and Synaptogenesis: A Study in Developing Mouse Intercostal Muscle

GUIDO J. JENNISKENS, THEO HAFMANS, JACQUES H. VEERKAMP, AND TOIN H. VAN KUPPEVELT*
Department of Biochemistry 194, University Medical Center, NCMLS, Nijmegen, The Netherlands

ABSTRACT **Formation of a basal lamina (BL) ensheathing developing skeletal muscle cells is one of the earliest events in mammalian skeletal muscle myogenesis. BL-resident heparan sulfate proteoglycans have been implicated in various processes during myogenesis, including synaptic differentiation. However, attention has focused on the proteoglycan protein core, ignoring the glycosaminoglycan moiety mainly because of a lack of appropriate tools. Recently, we selected a panel of anti–heparan sulfate antibodies applied here to study the spatiotemporal distribution of specific heparan sulfate (HS) epitopes during myogenesis. In mouse intercostal muscle at embryonic day (E14), formation of acetylcholine receptor clusters at synaptic sites coincides with HS deposition. Although some HS epitopes show a general appearance throughout the BL, one epitope preferably clusters at synaptic sites but does so only from E16 onward. During elongation and maturation of primary myotubes, a process preceding secondary myotube development, significant changes in the HS epitope constitution of both synaptic and extrasynaptic BL were observed. As a whole, the data presented here strengthen previous observations on developmental regulation by BL components, and add to the putative roles of specific HS epitopes in myogenesis and synaptogenesis.**

Key words: basal lamina; glycosaminoglycan; heparan sulfate proteoglycan; myogenesis; neuromuscular junction; synaptogenesis

INTRODUCTION

The synaptic cleft of the neuromuscular junction (NMJ) is occupied by a layer of extracellular material, which escheats all vertebrate skeletal muscle fibers: the basal lamina (BL). Several BL components are distributed in distinct synaptic and extrasynaptic regions, whereas others are common (Hall and Sanes, 1993). For many years, it has been recognized that BL-resident proteins play a regulating role in the differentiation and maintenance of both pre- and postsynaptic membranes (Burden, 1998; Meier and Wallace, 1998). Thus far, only few reports on the composition of the BL during myogenesis and synaptogenesis mention proteoglycans.

Proteoglycans are proteins that have a glycosaminoglycan (GAG) chain covalently attached to a core protein. In the case of heparan sulfate proteoglycans (HSPGs), the GAG moiety consists of heparan sulfate (HS), an unbranched chain of 30 to 150 disaccharides. Each HS disaccharide unit, consisting of a glucosamine and an uronic acid residue, can be modified by *N*-deacetylation, *N*-sulfation, 2-*O*-, 3-*O*-, and/ or 6-*O*-sulfation and C-5 epimerization. The concert of these modifications potentially makes HS a very information-dense biopolymer, to which several proteins may bind in a monosaccharide sequence-specific way (Salmivirta et al., 1996; Bernfield et al., 1999; Tumova et al., 2000; Turnbull et al., 2001; Gallagher, 2001). In developmental processes, however, the functions of HS have remained mostly underappreciated until recently (Perrimon and Bernfield, 2000).

In recent years, there have been several reports on the roles of BL-resident HSPGs in myogenesis and synaptogenesis. These include the roles of agrin in acetylcholine receptor (AChR) clustering (Ruegg and Bixby, 1998; Lin et al., 2001), the involvement of syndecan-2 in neural synaptogenesis (Hsueh et al., 1998), the binding of growth factors in NMJs by perlecan (Peng et al., 1998), the focal immobilization of BL-resident proteins like acetylcholine esterase (AChE) by perlecan (Peng et al., 1999), the involvement of perlecan in the assembly of laminin in the BL (Henry et al., 2001), and the maturation and maintenance of the NMJ and its synaptic BL by the dystrophin-glycoprotein complex and associated HSPGs (Grady et al., 2000; Jacobson et al., 2001).

Grant sponsor: Netherlands Organization for Scientific Research (NWO); Grant number: 902-27-184.
Dr. Jenniskens' present address is Division of Bioengineering and Environmental Health, Massachusetts Institute of Technology, Cambridge, MA 02139.
*Correspondence to: Toin van Kuppevelt, Department of Biochemistry 194, UMC, NCMLS, P.O. Box 9101, 6500 HB Nijmegen, The Netherlands. E-mail: a.vankuppevelt@ncmls.kun.nl
Received 18 February 2002; Accepted 21 June 2002
DOI 10.1002/dvdy.10138

As early as 1984, it was shown that synaptic and extrasynaptic parts of the muscle BL are subject to dynamic changes during synaptogenesis (Chiu and Sanes, 1984). More specific, expression of two HS-related epitopes (David et al., 1992), perlecan (Larraín et al., 1997a), alternatively spliced isoforms of agrin (Hoch et al., 1993), the HSPG-families of the syndecans (Bernfield et al., 1993; Larraín et al., 1997b; Sogos et al., 1998) and glypicans (Brandan et al., 1996; Litwack et al., 1998), the proteoglycans decorin (Velleman et al., 1999), and SPOCK (Charbonnier et al., 2000; Cifuentes-Diaz et al., 2000) have been shown to be developmentally regulated. Olguin and Brandan recently reported the temporal and spatial coexpression of HSPGs syndecan-3 and decorin with myogenin, a transcription factor responsible for the induction of terminal skeletal muscle differentiation (Olguin and Brandan, 2001). Moreover, Nurcombe and coworkers found evidence for differential glycosylation of a HSPG core protein during murine neural cell differentiation (Nurcombe et al., 1993; Brickman et al., 1998). HS structure itself is also subject to regulation during development and aging in vivo (Feyzi et al., 1998; Guimond et al., 2001). Taken together, HSPGs and especially the sulfation patterns of the HS moiety are considered candidate regulators of developmental signaling (Lander, 1998; Selleck, 2000; Dhoot et al., 2001). However, much has to be learned about the distribution of specific HS epitopes during myogenesis in vivo and the roles of this class of glycosaminoglycans in developmental processes.

Recently, we reported on the selection of a panel of phage display-derived antibodies that recognize specific HS epitopes (Jenniskens et al., 2000). In the present study, we describe the spatiotemporal distribution of several HS epitopes during myogenesis in mouse intercostal muscle, and their distribution with regard to developing synapses. For the first time, specific HS epitopes of the cellular HS constitution are shown to be subject to a dynamic distribution during myogenesis and synaptogenesis in vivo.

RESULTS

Histogenesis of Mouse Intercostal Muscle

Intercostal muscle was chosen for studying muscle development and synaptogenesis, because its muscle mass is relatively homogeneous, well innervated, and easy to monitor (Theiler, 1989; Hogan et al., 1994). To improve the comparability between intercostal muscles of different developmental stages, we focused our study on the *m. intercostalis externus* between ribs 5 and 6.

Intercostal muscles are divided in two main musclemasses: *m. intercostalis internus* and *m. intercostalis externus* (Fig. 1). The *m. intercostalis internus* is located at the internal side and has a function in drawing adjacent ribs together during forced expiration. The *m. intercostalis externus* is located at the external side and elevates adjacent ribs during inspiration. During late-embryogenesis, we observed an asynchronous development of these intercostal muscles. From cranial to caudal, the *m. intercostalis externus* showed a more pronounced differentiation, compared with the *m. intercostalis internus*. Whereas the latter consisted of a relatively heterogeneous population of loosely dispersed small muscle fibers, the *m. intercostalis externus* showed a more organized homogeneous distribution of fibers with a larger diameter. Moreover, the *m. intercostalis externus* contained more nerve bundles and blood vessels in corridors of perimysial connective tissue. The observed differences got more pronounced during the course of embryogenesis.

Localization of HS Epitopes

Information about the anti-HS antibodies and their corresponding epitopes is given in Table 1. Localization of individual epitopes is depicted in Figures 2–7 and is summarized in Table 2.

12 and 13 Days In Utero

At early developmental stages, intercostal muscle masses were scarcely detectable as such, when using immunohistochemical methods to stain for HS. Muscle primordia, at these stages, consist of fibroblasts and mononucleated myoblasts, the latter fusing to form primary myotubes. Upon myoblast fusion, patches of extracellular matrix material are formed on the myotube surface. Ongoing deposition of extracellular material results in the formation of a continuous BL in the following days. Except for RB4EA12, the antibodies used in this study showed a faint, granular staining of extracellular material in myogenic regions. Control antibody MPB01 showed no staining whatsoever in all developmental stages examined.

14 Days In Utero

At 14 days in utero, the intercostal muscle appeared as a relatively loosely dispersed muscle mass. Nuclei were relatively large and located in the center of the myotubes. Blood vessels and nerve bundles were located in connective tissue surrounding myogenic areas.

BL formation had progressed to a nearly continuous sheet, which could be stained with anti-HS antibodies AO4B05 (Fig. 2a), AO4B08 (Fig. 3a), RB4CB9, and, to a lesser extent, RB4CD12 (Fig. 4a). The HS epitope recognized by AO4B05 was present throughout the newly formed BL. AO4B05 staining was slightly more

Abbreviations

AChE	acetylcholinesterase
AChR	acetylcholine receptor
BL	basal lamina
e-c coupling	excitation-contraction coupling
GAG	glycosaminoglycan
HS	heparan sulfate
HSPG	heparan sulfate proteoglycan
NMJ	neuromuscular junction
vgNa^+channel	voltage-gated sodium channel

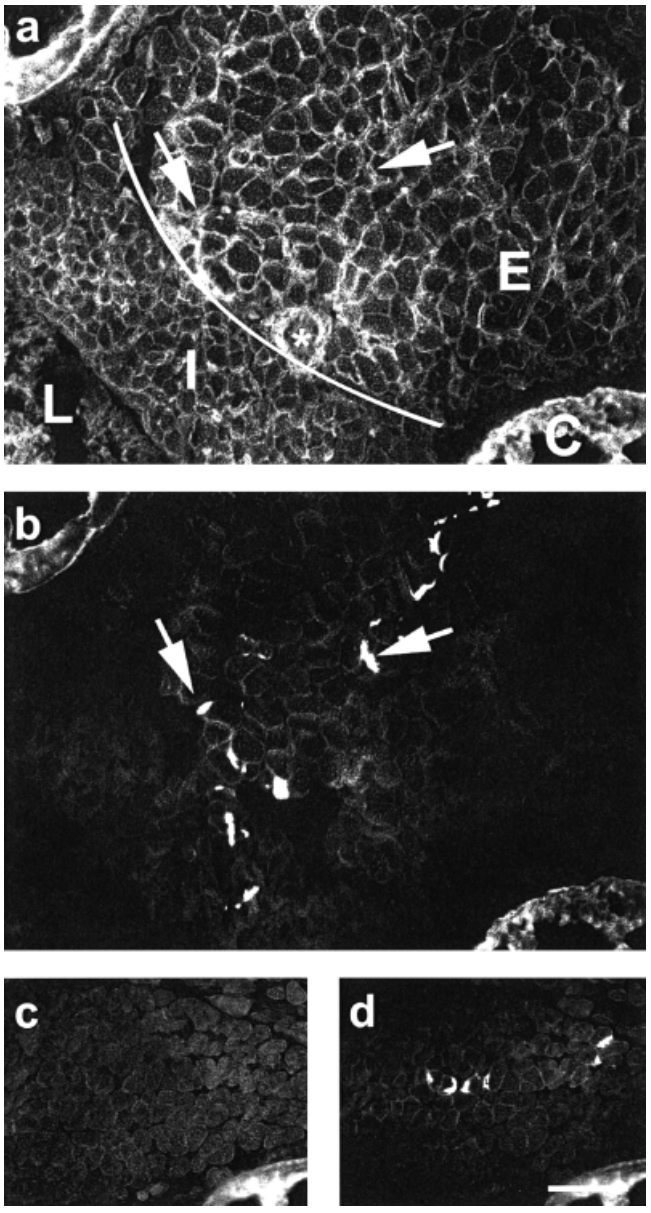

Fig. 1. Overview of *m. intercostalis internus* and *m. intercostalis externus* at E20 (birth). The cryosection was stained with an anti–heparan sulfate (HS) antibody (**a**), control antibody MPB01 (**c**), and α-bungarotoxin (**b,d**). HS epitopes are localized in both extrasynaptic and synaptic basal laminae (arrows in a), as well as in perimysial structures including nerves (asterisk in a) and blood vessels. The curved line marks the border between the *m. intercostalis internus* (I in a), which consists of a relatively heterogeneous population of loosely dispersed small muscle fibers, and the *m. intercostalis externus* (E in a) comprising a more homogeneous set of muscle fibers with a larger diameter. b: Note that neuromuscular junctions are positioned in the center of the intercostal muscle mass. c: Non-HS control antibody MPB01 does not stain any extracellular structure. The ribs (costa; C in a) in the upper left-hand (a,b) and lower right-hand corners (a–d) are visible because of high levels of autofluorescence. L, lung. Scale bar in d = 25 μm in a,b, 50 μm in c,d.

intense at some sites of AChR aggregation. Antibodies AO4B08 and RB4CB9 showed a more granular staining of the BL. Antibody RB4EA12 (Fig. 5a) did not stain muscle BL but was present in small intracellular granules.

Consistent with reports in literature, AChR clustering was first visible at embryonic day (E14). The voltage-gated sodium channel (vgNa$^+$channel), another postsynaptic ion channel involved in excitation-contraction coupling (e-c coupling), showed a uniform distribution over the myotube membrane, with a decrease in density at AChR clusters (Fig. 6a).

16 Days In Utero

The diameter of the myotubes had increased by E16. Also, muscle masses were more compact and clusters of myotubes were separated by septa of connective tissue containing nerve bundles and blood vessels. In general, nuclei were smaller and were located either centrally or eccentrically, forming a heterogeneous set of multinucleated myotubes. The *m. intercostalis internus* and *m. intercostalis externus* were distinguishable, which enabled us to focus on the latter from this developmental stage onward.

Antibodies AO4B05 (Fig. 2b), AO4B08 (Fig. 3b), RB4CB9, and RB4CD12 (Fig. 4b) stained the entire muscle BL. AO4B08 and RB4CB9 predominantly stained the muscle BL, whereas RB4CD12 epitopes were also present in blood vessels and in nerves located in the perimysium. RB4EA12 (Fig. 5b) continued to stain perinuclear granules but stained also, faintly, at sites of AChR clustering. vgNa$^+$channels (Fig. 6b) showed a modest overall distribution over the myotube membrane at this stage.

18 Days In Utero

By 18 days in utero, myotube diameter had further increased. Myotubes had become more homogeneous, both in size and in shape, approaching the regular pattern of mature muscle. Myonuclei were predominantly located eccentrically, although central nuclei could be observed occasionally.

Antibodies AO4B05 (Fig. 2c), AO4B08 (Fig. 3c), RB4CB9, and RB4CD12 (Fig. 4c) stained the muscle BL in a way comparable to that seen in 16-day fetuses. RB4EA12 (Fig. 5c) failed to stain cytosolic granules as well as the extrasynaptic BL, but showed a distinct staining of the synaptic BL. The vgNa$^+$channel (Fig. 6c) continued to be evenly distributed over the sarcolemma.

20 Days In Utero/Birth

At birth, the *m. intercostalis externus* appeared more homogeneous and densely packed when compared with earlier developmental stages. This uniform maturation state is in line with the distribution of AO4B05 (Fig. 2d), AO4B08 (Fig. 3d), RB4CB9, and RB4CD12 (Fig. 4d) epitopes that stained the entire muscle BL. RB4EA12 (Fig. 5d) stained the extrasynaptic BL only to a minor extent, whereas a strong signal was achieved for synaptic and nerve BL. vgNa$^+$channels

TABLE 1. Complementarity-Determining Region 3 (CDR3) Sequences and Preferred HS Sequences of the Anti-HS Antibodies Used in This Study[a]

Antibody	CDR3 sequence	Preferred HS binding sequence
AO4B05	LKQQGIS	ND
AO4B08	SLRMNGWRAHQ	GlcNS6S-IdoUA2S-GlcNS6S[b]
RB4CB9	HAPLRNTRTNT	[c]
RB4CD12	GMRPRL	GlcNS6S-IdoUA2S-GlcNS6S[b]
RB4EA12	RRYALDY	GlcNS6S-IdoUA-GlcNS6S
MPB01	PKRTRN	Not reactive with HS

[a]CDR3 sequences are shown in single-letter amino acid code. The preferred heparan sulfate (HS) sequence was deduced as described in Dennissen et al., 2002. Antibodies RB4CB9 and RB4CD12 (previously selected against human skeletal muscle glycosaminoglycans) are identical to HS4E4 and HS4D4 (selected against a kidney HS preparation), respectively. ND, not determined.
[b]Antibodies AO4B08 and RB4CD12 recognize different HS epitopes, as deduced by their differential reactivity in enzyme-linked immunosorbent assay and different staining patterns in muscle and kidney (Jenniskens et al., 2000; Dennissen et al., 2002).
[c]Preferred sequence is not known, N-sulfation is indispensible, 6-O sulfation is likely to be inhibitory.

TABLE 2. Immunostaining of the Antibodies Used in This Study During Myogenesis[a]

Antibody	E12-13	E14	E16	E18	E20	P2	Adult
AO4B05	+/−, gr	++, c	++, c	++, c	++, c	++, c	++, c
AO4B08	+/−, gr	++, gr	++, c	++, c	++, c	++, c	++, c
RB4CB9	+/−, gr	++, gr	++, c	++, c	++, c	++, c	++, c
RB4CD12	+/−, gr	+, gr	++, c	++, c	++, c	++, c	++, c
RB4EA12	−	−[b]	+/−[bc]	+[c]	++[c]	++[c]	++[c]
MPB01[d]	−	−	−	−	−	−	−

[a]Transverse sections of intercostal muscle at embryonic day (E)12, E13, E14, E16, E18, E20, and postnatal day 2 (P2), as well as adult *m. soleus* were stained for various heparan sulfate epitopes and for acetylcholine receptor clusters. Immunostaining patterns of the antibodies presented in this study are summarized with regard to muscle basal lamina (BL) reactivity. Staining intensity: ++, strong; +, moderate; +/−, weak; −, absent (n = 5). gr, granular staining of the BL; c, continuous staining of the BL.
[b]Staining of small intracellular granules.
[c]Predominant staining of the synaptic BL.
[d]Control antibody.

(Fig. 6d) were homogeneously distributed over the myotube membrane.

2 Days Postnatal

During early postnatal development, no major changes were observed in the distribution of HS epitopes: AO4B05 (Fig. 2e), AO4B08 (Fig. 3e), and RB4CB9 stained the entire BL. The RB4CD12 epitope (Fig. 4e) was evenly distributed over the muscle BL, but was more abundant in neural and capillary BL. RB4EA12 (Fig. 5e) was predominant in synaptic and neural BL. vgNa$^+$channels (Fig. 6e) were homogeneously distributed over the cell membrane.

Adult

After fetal development, staining patterns of the HS epitopes studied did not undergo major changes with regard to BL location. Confocal imaging of the NMJs of *m. soleus* enabled us to visualize differences in the location of individual HS epitopes with regard to AChR clusters. Most antibodies stained the entire BL and were located separate from AChR clusters, as exemplified by AO4B08 (Fig. 7a1–c1). RB4EA12 (Fig. 7a2–c2), however, showed a tight colocalization with AChR clusters.

DISCUSSION

Skeletal muscle tissue is derived from embryonic mesenchyme of the somites (Grinnel, 1995). During early mouse embryogenesis, organ primordia are established, followed by organogenesis from E10 until E14 and subsequent fetal growth and development (Hogan et al., 1994). In *extensor digitorum longus* muscle at E12, motor nerves reach muscle primordia, which already contain some multinucleate primary myotubes surrounded by myoblasts. Primary myotubes are elongated by myoblast fusion during 2 days, after which myogenesis resumes with the generation of secondary myotubes. The second generation of myotubes is formed on the scaffold of primary myotubes between E14 and E16. This biphasic character of myotube development is thought to be caused by the necessity of primary myotubes to first reach a certain stage of maturation, including sarcolemmal changes, before secondary myotube development can be supported (Ontell and Kozeka, 1984; Jansen and Fladby, 1990). Extracellular

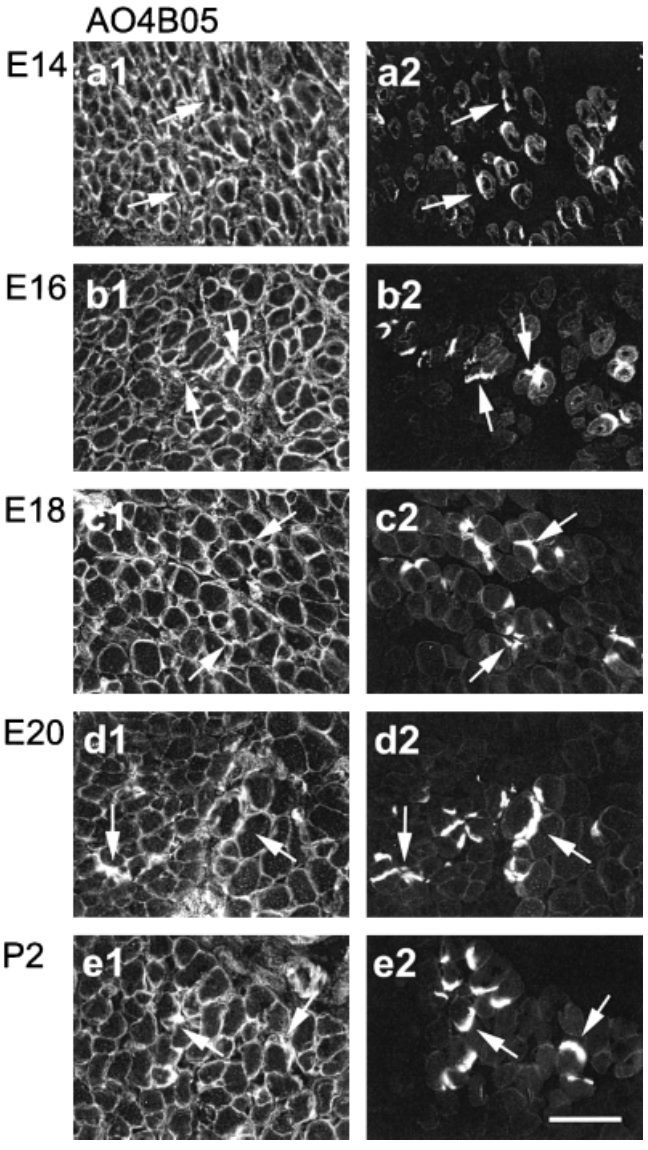

Fig. 2. Staining of developing skeletal muscle with antibody AO4B05. Transversal sections of intercostal muscle at embryonic day(E) 14 (**a**), E16 (**b**), E18 (**c**), E20 (**d**), and postnatal day 2 (**e**) were stained for HS epitope AO4B05 (a1–e1) and acetylcholine receptor (a2–e2). The AO4B05 heparan sulfate (HS) epitope is present in newly formed basal lamina (BL), both in synaptic (arrows) and in extrasynaptic BL. Scale bar = 25 μm.

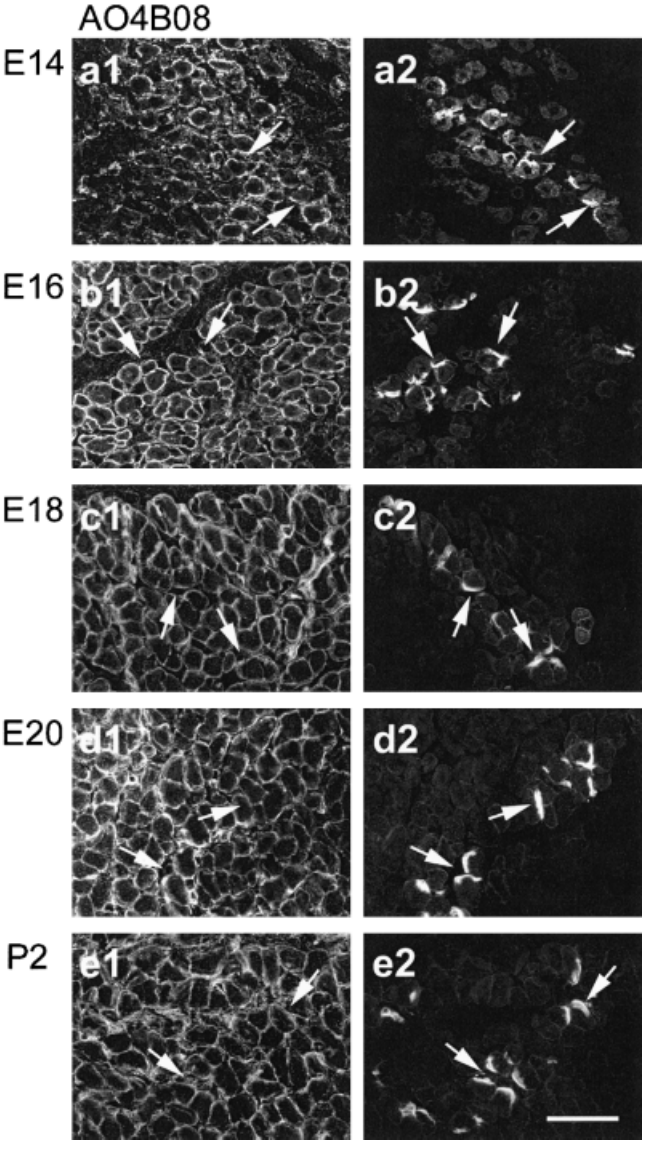

Fig. 3. Staining of developing skeletal muscle with antibody AO4B08. Transverse sections of intercostal muscle at embryonic day (E) 14 (**a**), E16 (**b**), E18 (**c**), E20 (**d**), and postnatal day 2 (**e**), stained for heparan sulfate (HS) epitope AO4B08 (a1–e1) and acetylcholine receptor (a2–e2). At E14, the AO4B08 HS epitope is present in basal lamina (BL) in a granular distribution in synaptic areas (a, arrows) as well as in extrasynaptic areas. From E16 onward, the HS epitope is homogeneously distributed throughout the BL, irrespective of synapses (b–e, arrows). Scale bar = 25 μm.

material is deposited on the myotube surface, beginning on E14, to form a continuous BL by E19 (Chiu and Sanes, 1984).

One of the HS epitopes examined in this study (AO4B05) surrounds primary myotubes in a relatively continuous staining at the onset of BL formation, at E14. Other HS epitopes that are also present throughout the muscle BL (AO4B08, RB4CB9, and RB4CD12) show a less continuous, granular distribution. Thus, a specific HS epitope is present in a more or less continuous sheet surrounding primary myoblasts before BL completion, whereas other HS epitopes are deposited in the course of BL formation. Because BL formation during maturation of primary myotubes may be causal for the onset of generation of secondary myotubes, we suspect significant roles for individual HS epitopes in the formation and integrity of developmental stage-specific BL. Deposition and accumulation of certain HS epitopes, both qualitatively and quantitatively, may combine to form a BL capable of directing developmen-

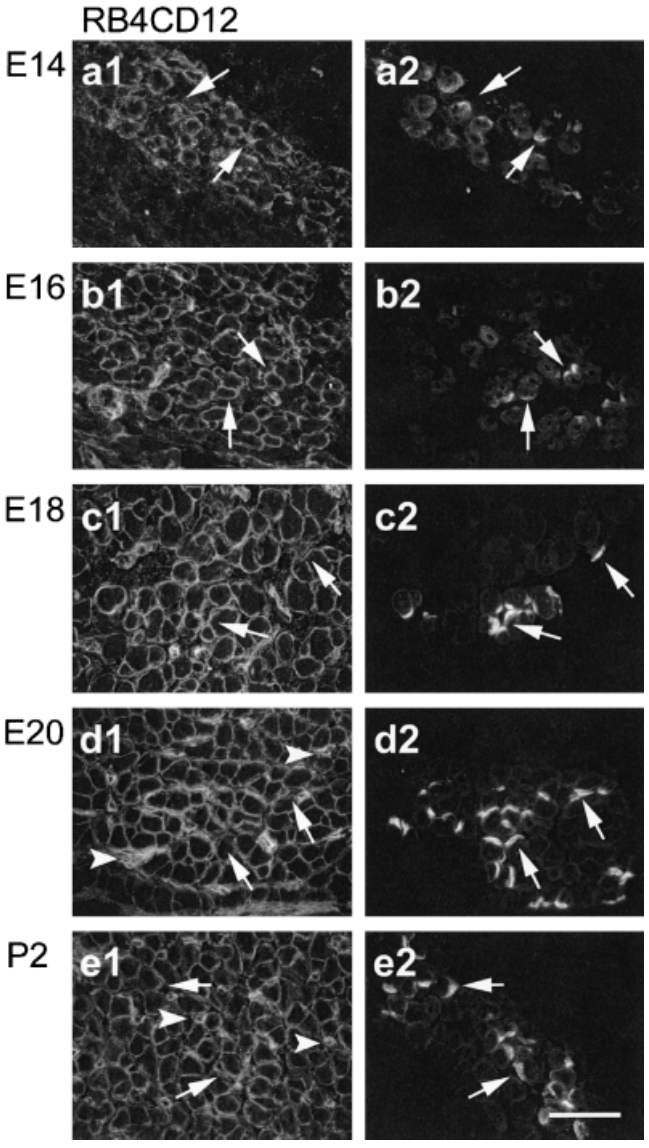

Fig. 4. Staining of developing skeletal muscle with antibody RB4CD12. Transversal sections of intercostal muscle at embryonic day (E) 14 (**a**), E16 (**b**), E18 (**c**), E20 (**d**), and postnatal day 2 (**e**), stained for heparan sulfate (HS) epitope RB4CD12 (a1–e1) and acetylcholine receptor (a2–e2). Although present in a granular distribution at E14 (a), HS epitope RB4CD12 is evenly distributed in muscle basal laminae (BL) during development (b–e). Compared with synaptic (arrows) and extrasynaptic BL, a more intense staining was achieved for blood vessels and nerves present in perimysial connective tissue (arrowheads). Scale bar = 25 μm.

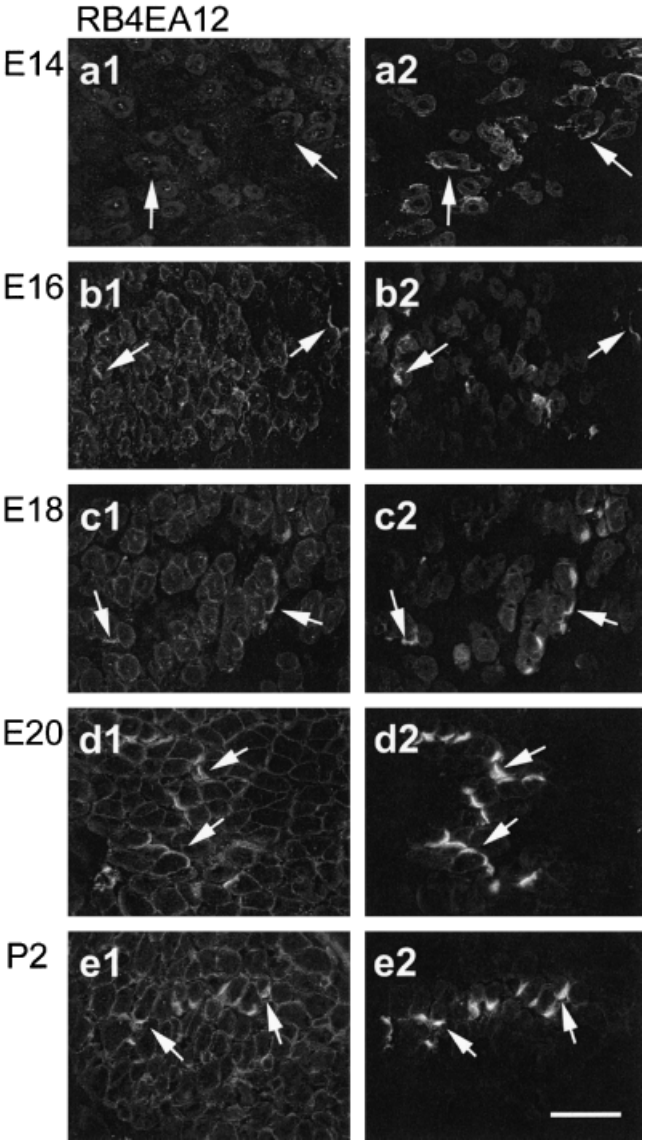

Fig. 5. Staining of developing skeletal muscle with antibody RB4EA12. Transverse sections of intercostal muscle at embryonic day (E) 14 (**a**), E16 (**b**), E18 (**c**), E20 (**d**), and postnatal day 2 (**e**), stained for heparan sulfate (HS) epitope RB4EA12 (a1–e1) and acetylcholine receptor (a2–e2). a: At 14 days in utero, HS epitope RB4EA12 could be detected in small perinuclear granules (a, arrows), whereas it was not present in muscle basal laminae (BL) at all. During myogenic differentiation, staining for this HS epitope was poor and granular in extrasynaptic BL but abundant in the synaptic portion of the BL (b–e, arrows) and nerve BL. Scale bar = 25 μm.

tal processes. Moreover, spatial differences in the density of specific HS epitope deposits may be causal for the induction of local adaptations, such as synaptic specializations.

AChR clustering at sites of neuromuscular contact first occurs approximately on day E14. At this time, the synaptic cleft already contains BL material (Nakajima et al., 1980), of which the HSPG agrin is involved in the clustering of AChR (Ruegg and Bixby, 1998). During fetal growth, a faint staining of AChRs in the extrasynaptic cell membrane is observed, as well as a stronger cytosolic staining of this protein in and around synaptic areas (see, e.g., Fig. 2a2–e2). This elevated staining may be due to higher expression levels of AChR from synaptic nuclei. Newly formed AChRs are detected in the cytosol, most probably located within Golgi vesicles while being transported to the sarcolemma, and in the cell membrane before clustering at synaptic sites. Spe-

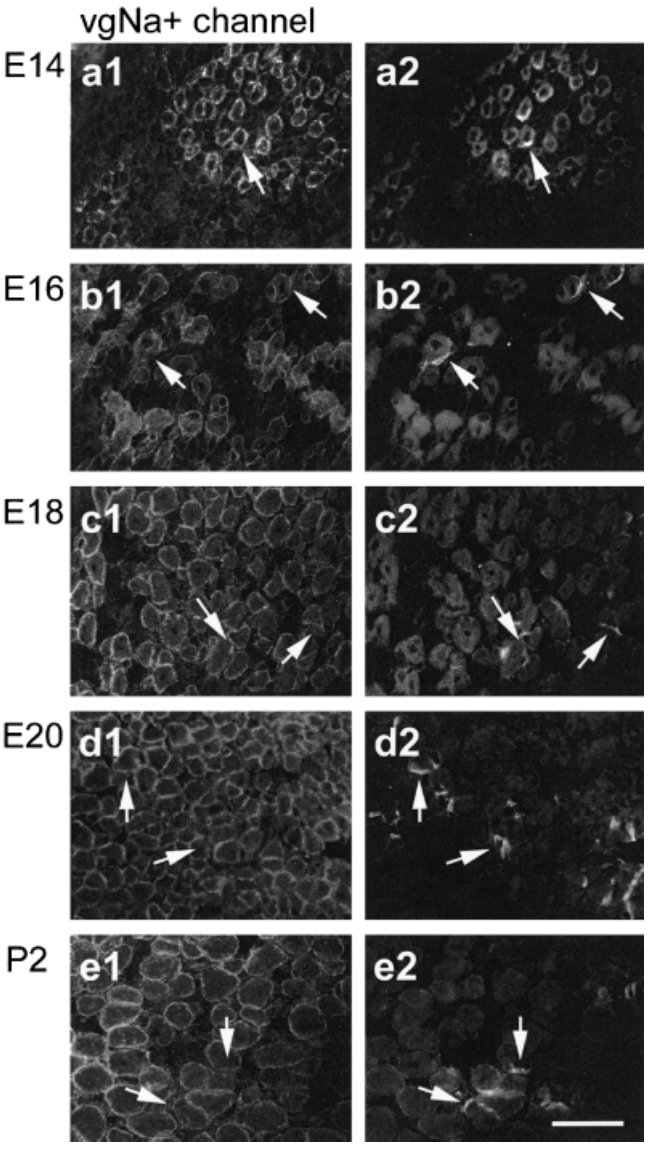

Fig. 6. Staining of developing skeletal muscle with an antibody against voltage-gated sodium ($vgNa^+$) channels. Transversal sections of intercostal muscle at embryonic day (E) 14 (**a**), E16 (**b**), E18 (**c**), E20 (**d**), and postnatal day 2 (**e**), stained for $vgNa^+$channel (a1–e1) and acetylcholine receptor (a2–e2). $vgNa^+$channels, which are located in the muscle plasma membrane, could be visualized as early as E14, the stage in which acetylcholine receptor clustering occurs (a, arrows). In all stages of muscle development, these ion channels were evenly distributed in the membrane, apart from a slight decrease in density in synapses (a–e, arrows). Scale bar = 25 μm.

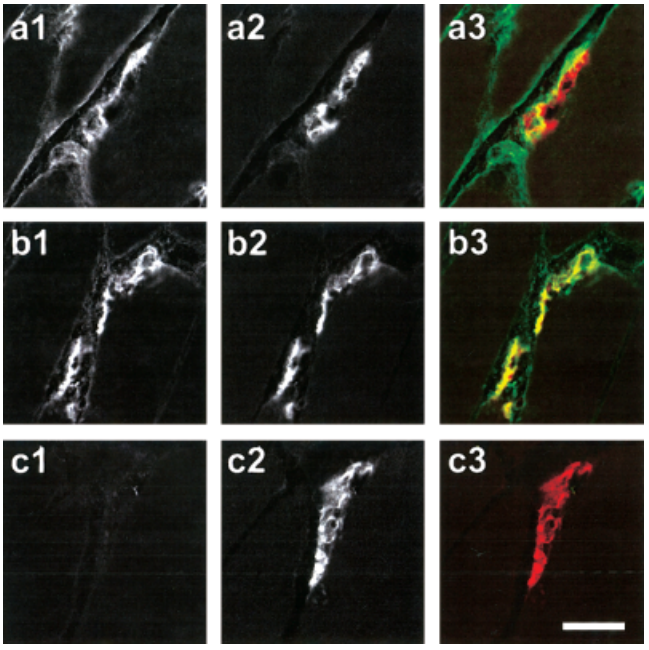

Fig. 7. Comparison of the distribution of heparan sulfate (HS) epitopes AO4B08 and RB4EA12 at synaptic sites. Confocal images of sections through neuromuscular junctions of adult *m. soleus* stained for AO4B08 (**a1**), RB4EA12 (**b1**), control antibody MPB01 (**c1**), and acetylcholine receptor (AchR; **a2,b2,c2**). Merged images are shown in color (**a3,b3,c3**). HS epitope AO4B08 is present throughout the endomysial basal laminae (BL), including synaptic regions (**a1,a3**). In contrast, HS epitope RB4EA12 is hardly present in the extrasynaptic BL but enriched in synapses, where it colocalizes tightly with AChR clusters (b1,b3). Control antibody MPB01 does not stain muscle BL at all (c1,c3). Scale bar = 50 μm.

cializations of the synaptic regions take place during the days of myogenesis after E14. A few days postnatally, these alterations culminate in functional neuromuscular junctions containing a continuous sBL, a thickened postsynaptic membrane, and junctional folds. One of the prominent features of the developing NMJ, the accumulation of AChE, is detectable soon after AChR clustering; nearly all junctional areas are rich in AChE by E18 (Chiu and Sanes, 1984). This process is mediated by BL-resident dermatan sulfate proteoglycans and HSPGs (Brandan et al., 1985; von Bernhardi and Inestrosa, 1990), including perlecan (Peng et al., 1999).

The most striking staining pattern was observed for HS epitope RB4EA12, which preferably clusters at synaptic sites by E16 and accumulates at these locations thru E20. AO4B05, AO4B08, and RB4CB9 are present in the sBL as early as E14, during the onset of AChR clustering. Such regulated appearance of HS epitopes simultaneous with the aggregation of synapse-specific proteins is indicative of a possible involvement of these HS epitopes in the processes involved. The late appearance of RB4EA12 and its persisted synaptic location in adult tissue, occur parallel to the clustering and retention of AChE in sBL However, this HS epitope colocalizes tightly with AChR clusters that are located in the postsynaptic membrane. This finding may indicate that HS epitope RB4EA12 is possibly present in cell surface HSPGs like glypicans and syndecans, rather than in BL-resident HSPGs like agrin and perlecan. It should be noted, however, that a single HS chain can be up to 100 nm in length and, therefore, is able to span the entire synaptic cleft regardless of the location of the protein core. Other HS epitopes show a distinct spatio-

temporal distribution with regard to AChR clusters and vgNa^+channels but stain the entire BL surrounding the muscle fibers. At present, we have no information as to a possibly restricted occurrence of unique HS epitopes on specific proteoglycans. Defining the HS epitope profiles of individual core proteins forms a major challenge for future studies.

Polypeptide growth factors, like epidermal growth factor, fibroblast growth factor-2, insulin-like growth factors, and transforming growth factor-β, play key roles in myogenesis (McCusker and Clemmons, 1994). Some of the growth factors are known to interact with HS or heparin. Fibroblast growth factors, for instance, regulate the growth and differentiation of embryonic primary myoblasts (Itoh et al., 1996; Flanagan-Steet et al., 2000) as well as secondary and adult myoblasts (Flanagan-Steet et al., 2000). Moreover, fibroblast growth factor-2 is involved in both presynaptic (Dai and Peng, 1995) and postsynaptic (Peng et al., 1991) differentiation. Therefore, we studied the spatiotemporal distribution of several growth factors (epidermal growth factor, fibroblast growth factor-2, insulin-like growth factor, and transforming growth factor-β), with regard to the HS epitopes studied here. We were unable to detect correlations between the distribution of either of these growth factors with regard to the distribution patterns of the HS epitopes (data not shown). In future studies, it will be interesting to determine any potential interactions between HS-binding growth factors and the HS epitopes defined by the antibodies studied here. Such studies require a more biochemical approach and would significantly contribute to our understanding of the mechanisms underlying growth factor mediated processes.

In recent years, it has become widely accepted that especially the sulfation pattern of HS domains regulates specific interactions with HS-binding proteins (Bernfield et al., 1999; Tumova et al., 2000). Binding of fibroblast growth factor-2 requires 2-*O* sulfation of iduronic acid residues, whereas additional 6-*O* sulfation of the glucosamine residue is required for the binding of fibroblast growth factor-1 (Kreuger et al., 2001). Previously, carbohydrates (e.g., *N*-acetylated galactosamine) were shown to be primarily located in the sBL and differentially located within the synapse, on the basis of lectin and antibody-binding profiles (Sanes and Cheney, 1982; Iglesias et al., 1992; Martin et al., 1999). By regulating the structure of HS and the spatiotemporal distribution of specific HS epitopes, the muscle and the innervating nerve may create a specific microenvironment, which attracts and sequesters HS binding proteins necessary for the correct development of the NMJ.

Synaptic development is a lifelong process rather than an embryonic event. NMJs persist for a lifetime but undergo structural and functional changes due to a dynamic equilibrium that permits remodeling in response to alterations in activity (reviewed by Sanes and Lichtman, 1999). After fetal development, HS is also shown to be subject to age-related changes (Feyzi et al., 1998).

In summary, considering the tight and dynamic regulation of HSPG expression during myogenesis, we looked in detail to the occurrence of specific HS epitopes. Our results indicate a highly regulated spatiotemporal expression of various HS epitopes during muscle development. The results presented in this study argue for roles of individual HS epitopes in developmental processes underlying myogenesis and synaptogenesis.

EXPERIMENTAL PROCEDURES

Materials

C3H mice were obtained from the University of Nijmegen Central Animal Laboratory. All chemicals used were from Merck (Darmstadt, Germany), unless stated otherwise. Bovine serum albumin (fraction V) and NaN_3 were obtained from Sigma (St. Louis, MO). Target Unmasking Fluid was purchased from Boehringer Mannheim (Mannheim, Germany), and anti-pan sodium channel rabbit polyclonal immunoglobulin (Ig) G (SP19) from Alomone Labs (Jerusalem, Israel). Anti–c-*Myc* tag goat polyclonal IgG (A-14) was from Santa Cruz Biotechnology (Santa Cruz, CA). Alexa 488–conjugated donkey anti-goat IgG, goat anti-rabbit IgG, and Alexa 594–conjugated α-bungarotoxin were purchased from Molecular Probes (Eugene, OR). Mowiol (4-88) was obtained from Calbiochem (La Jolla, CA).

Anti-HS Antibodies

Preparation of anti-HS antibodies (periplasmic fractions) AO4B05, AO4B08, RB4CD12, RB4EA12, and control antibody MPB01 was performed as described (Jenniskens et al., 2000). Antibody MPB01 was randomly selected from scFv library #1. This antibody is a member of V_H family 3, has DP segment 38, bears the complementarity-determining region 3 (CDR3) sequence PKRTRN (single-letter amino acid code), and is not reactive with HS or heparin from any source tested, as analyzed by enzyme-linked immunosorbent assay and immunofluorescence assay (IFA) techniques.

Pre- and Postnatal Mouse Tissue

C3H mice were bred under standard conditions and monitored for vaginal plugs twice a day. The first day of occurrence of a vaginal plug was taken as day 0 of gestation (E0). Pregnant mice were quarantined and kept solitary until the litter had reached the indicated E-number (12, 13, 14, 15, 16, 17, 18, and 20 days in utero). Mice were anesthetized and killed by cervical dislocation, in accordance with the ethic regulations of the university. Embryos were isolated either with (E12 and 13) or without (E14–E20) the surrounding uteric tissue, rinsed in phosphate buffered saline (PBS), snap-frozen in liquid nitrogen-cooled isopentane, and stored at −80°C. Birth occurred on average at day E20 (P0). Mice of postnatal day 2 (P2) were anesthetized before freezing. For each developmental stage, at least

three individual mice, derived from two separate litters, were studied. Adult intercostal muscles were difficult to isolate in a way appropriate for cryosectioning, because of the presence of osteofied ribs. Therefore, we used specimens of the *m. soleus*, isolated from the pregnant females that were killed, for studying adult NMJs.

Immunohistochemistry

Five- to 10-μm-thick cryosections of whole embryos, newborns, or adult tissue specimens were cut, mounted on slides, dried thoroughly, and stored at −80°C until use. Cryosections were rehydrated in PBS for 10 min. After 20 min blocking in PBS containing 0.1% (w/v) BSA, cryosections were incubated with anti-heparan sulfate antibodies for 90 min. Bound antibodies were visualized by using anti–c-*Myc* goat polyclonal antibody A-14 and Alexa 488–conjugated donkey anti-goat IgG (60 min each). AChR clusters were stained by Alexa 594–conjugated α-bungarotoxin, included in the final incubation. Primary antibodies against voltage-gated ion channel were applied for 60 min, after which bound antibodies were visualized by using Alexa 488–conjugated goat anti-rabbit IgG for 60 min. After each incubation, cryosections were washed three times 10 min with PBS. Finally, cryosections were fixed in 100% methanol, dried, and embedded in Mowiol (10% [w/v] in 0.1 M Tris-HCl, pH 8.5/ 25% [v/v] glycerol/ 2.5% [w/v] NaN_3). As a control, primary, secondary, or conjugated antibodies were omitted. Also, a control phage display-derived scFv antibody that does not react with HS was used (MPB01). To investigate the possibility of epitope masking by tissue-resident HS-binding proteins, cryosections were incubated in high-salt buffer (PBS/ 1 M NaCl) or in Target Unmasking Fluid before immunostaining. Because no apparent changes in staining patterns were observed, we assume that the procedure described here allows for the staining of all HS epitopes present in the tissue. All incubations were performed at ambient temperature (21°C). Photographs were taken by using a constant shutter time on a Zeiss Axioskop immunofluorescence microscope (Göttingen, Germany). Confocal images were made on a Nikon Diaphot inverted microscope attached to a Bio-Rad MRC1024 ES confocal laser scanning microscope (Hemel Hempstead, UK). Digital images were processed by using Confocal Assistant 4.02 and Adobe Photoshop 6.0 software.

ACKNOWLEDGMENTS

We thank Toine Lamers for help with pilot experiments and Paul Jap for expert advice in histologic work and helpful discussions.

REFERENCES

Bernfield M, Hinkes MT, Gallo RL. 1993. Developmental expression of the syndecans: possible function and regulation. Development Suppl 205–212.

Bernfield M, Götte M, Park PW, Reizes O, Fitzgerald ML, Lincecum J, Zako M. 1999. Functions of cell surface heparan sulfate proteoglycans. Annu Rev Biochem 68:729–777.

Brandan E, Maldonado M, Garrido J, Inestrosa NC. 1985. Anchorage of collagen-tailed acetylcholinesterase to the extracellular matrix is mediated by heparan sulfate proteoglycans. J Cell Biol 101:985–992.

Brandan E, Carey DJ, Larraín J, Melo F, Campos A. 1996. Synthesis and processing of glypican during differentiation of skeletal muscle cells. Eur J Cell Biol 71:170–176.

Brickman YG, Ford MD, Gallagher JT, Nurcombe V, Bartlett PF, Turnbull JE. 1998. Structural modification of fibroblast growth factor-binding heparan sulfate at a determinative stage of neural development. J Biol Chem 273:4350–4359.

Burden SJ. 1998. The formation of neuromuscular synapses. Genes Dev 12:133–148.

Charbonnier F, Chanoine C, Cifuentes-Diaz C, Gallien CL, Rieger F, Alliel PM, Périn JP. 2000. Expression of the proteoglycan SPOCK during mouse embryo development. Mech Dev 90:317–321.

Chiu AY, Sanes JR. 1984. Development of basal lamina in synaptic and extrasynaptic portions of embryonic rat muscle. Dev Biol 103: 456–467.

Cifuentes-Diaz C, Alliel PM, Charbonnier F, De La Porte S, Molgó J, Goudou D, Rieger F, Périn JP. 2000. Regulated expression of the proteoglycan SPOCK in the neuromuscular system. Mech Dev 94: 277–282.

Dai Z, Peng HB. 1995. Presynaptic differentiation induced in cultured neurons by local application of basic fibroblast growth factor. J Neurosci 15:5466–5475.

David G, Mei Bai X, Van Der Schueren B, Cassiman J-J, Van Den Berghe H. 1992. Developmental changes in heparan sulfate expression: in situ detection with mAbs. J Cell Biol 119:961–975.

Dennissen MABA, Jenniskens GJ, Pieffers M, Versteeg EMM, Petitou M, Veerkamp JH, van Kuppevelt TH. 2002. Large, tissue-regulated, domain diversity of heparan sulfates demonstrated by phage display antibodies. J Biol Chem 277:10982–10986.

Dhoot GK, Gustafsson MK, Ai X, Sun W, Standiford DM, Emerson CP Jr. 2001. Regulation of Wnt signalling and embryo patterning by an extracellular sulfatase. Science 293:1663–1666.

Feyzi E, Saldeen T, Larsson E, Lindahl U, Salmivirta M. 1998. Age-dependent modulation of heparan sulfate structure and function. J Biol Chem 273:13395–13398.

Flanagan-Street H, Hannon K, McAvoy MJ, Hullinger R, Olwin BB. 2000. Loss of FGF receptor-1 signalling reduces skeletal muscle mass and disrupts myofiber organization in the developing limb. Dev Biol 218:21–37.

Gallagher JT. 2001. Heparan sulfate: growth control with a restricted sequence menu. J Clin Invest 108:357–361.

Grady RM, Zhou H, Cunningham JM, Henry MD, Campbell KP, Sanes JR. 2000. Maturation and maintenance of the neuromuscular synapse: genetic evidence for roles of the dystrophin-glycoprotein complex. Neuron 25:279–293.

Grinnell AD. 1995. Dynamics of nerve-muscle interaction in developing and mature neuromuscular junctions. Physiol Rev 75:789–834.

Guimond S, Turner K, Kita M, Ford-Perriss M, Turnbull J. 2001. Dynamics of heparan sulphate sequences in developing mouse brain: a potential regulatory mechanism during development. Biochem Soc Trans 29:177–181.

Hall ZW, Sanes JR. 1993. Synaptic structure and development: the neuromuscular junction. Cell 72(suppl):99–121.

Henry MD, Satz JS, Brakebusch C, Costell M, Gustafsson E, Fässler R, Campbell KP. 2001. Distinct roles for dystroglycan, β1 integrin, and perlecan in cell surface laminin organization. J Cell Sci 114: 1137–1144.

Hoch W, Ferns M, Campanelli JT, Hall ZW, Scheller RH. 1993. Developmental regulation of highly active alternatively spliced forms of agrin. Neuron 11:479–490.

Hogan B, Beddington R, Costantini F, Lacy E. 1994. Summary of mouse development. In: Manipulating the mouse embryo. New York: Cold Spring Harbor Laboratory Press. p 21–113.

Hsueh Y-P, Yang F-C, Kharazia V, Naisbitt S, Cohen AR, Weinberg RJ, Sheng M. 1998. Direct interaction of CASK/LIN-2 and syndecan

heparan sulfate proteoglycan and their overlapping distribution in neuronal synapses. J Cell Biol 142:139–151.
Iglesias M, Ribera J, Esquerda JE. 1992. Treatment with digestive agents reveals glycoconjugates specifically associated with rat neuromuscular junction. Histochemistry 97:125–131.
Itoh N, Mima T, Mikawa T. 1996. Loss of fibroblast growth factor receptors is necessary for terminal differentiation of embryonic limb muscle. Development 122:291–300.
Jacobson C, Côté PD, Rossi SG, Rotundo RL, Carbonetto S. 2001. The distroglycan complex is necessary for stabilization of acetylcholine receptor clusters at neuromuscular junctions and formation of the synaptic basement membrane. J Cell Biol 152:435–450.
Jansen JKS, Fladby T. 1990. The perinatal reorganization of the innervation of skeletal muscle in mammals. Prog Neurobiol 34:39–90.
Jenniskens GJ, Oosterhof A, Brandwijk R, Veerkamp JH, van Kuppevelt TH. 2000. Heparan sulfate heterogeneity in skeletal muscle basal lamina: demonstration by phage display-derived antibodies. J Neurosci 20:4099–4111.
Kreuger J, Salmivirta M, Sturiale L, Gimenez-Gallego G, Lindahl U. 2001. Sequence analysis of heparan sulfate epitopes with regard to affinities for FGF-1 and FGF-2. J Biol Chem 176:30744–30752.
Lander AD. 1998. Proteoglycans: master regulators of molecular encounter? Matrix Biol 17:465–472.
Larraín J, Alvarez J, Hassell JR, Brandan E. 1997a. Expression of perlecan, a proteoglycan that binds myogenic inhibitory basic fibroblast growth factor, is down regulated during skeletal muscle differentiation. Exp Cell Res 234:405–412.
Larraín J, Cizmeci-Smith G, Troncoso V, Stahl RC, Cary DJ, Brandan E. 1997b. Syndecan-1 expression is down-regulated during myoblast terminal differentiation. J Biol Chem 272:18418–18424.
Lin W, Burgess RW, Dominguez B, Pfaff SL, Sanes JR, Lee K-F. 2001. Distinct roles of nerve and muscle in postsynaptic differentiation of the neuromuscular synapse. Nature 410:1057–1064.
Litwack ED, Ivins JK, Kumbasar A, Paine-Saunders S, Stipp CS, Lander AD. 1998. Expression of the heparan sulfate proteoglycan glypican-1 in the developing rodent. Dev Dyn 211:72–87.
Martin PT, Scott LJC, Porter BE, Sanes JR. 1999. Distinct structures and functions of related pre- and postsynaptic carbohydrates at the mammalian neuromuscular junction. Mol Cell Neurosci 13:105–118.
McCusker RH, Clemmons DR. 1994. Effects of cytokines on insulin-like growth factor-binding protein secterion by muscle cells in vitro. Endocrinology 134:2095–2102.
Meier T, Wallace BG. 1998. Formation of the neuromuscular junction: molecules and mechanisms. Bioessays 20:819–829.
Nakajima Y, Kidokoro Y, Klier FG. 1980. The development of functional neuromuscular junctions in vitro: an ultrastructural and physiological study. Dev Biol 77:52–72.
Nurcombe V, Ford MD, Wildschut JA, Bartlett PF. 1993. Developmental regulation of neural response to FGF-1 and FGF-2 by heparan sulfate proteoglycan. Science 260:103–106.
Olguin H, Brandan E. 2001. Expression and localization of proteoglycans during limb myogenic activation. Dev Dyn 221:106–115.
Ontell M, Kozeka K. 1984. The organogenesis of murine striated muscle: a cytoarchitectural study. Am J Anat 171:133–148.
Peng HB, Baker LP, Chen Q. 1991. Induction of synaptic development in cultured muscle cells by basic fibroblast growth factor. Neuron 6:237–246.
Peng HB, Ali AA, Daggett DF, Rauvala H, Hassell JR, Smalheiser NR. 1998. The relationship between perlecan and dystroglycan and its implication in the formation of the neuromuscular junction. Cell Adhes Commun 5:475–489.
Peng HB, Xie H, Rossi SG, Rotundo RL. 1999. Acetylcholinesterase clustering at the neuromuscular junction involves perlecan and dystroglycan. J Cell Biol 145:911–921.
Perrimon N, Bernfield M. 2000. Specificities of heparan sulphate proteoglycans in developmental processes. Nature 404:725–728.
Ruegg MA, Bixby JL. 1998. Agrin orchestrates synaptic differentiation at the vertebrate neuromuscular junction. Trends Neurosci 21:22–27.
Salmivirta M, Lidholt K, Lindahl U. 1996. Heparan sulfate: a piece of information. FASEB J 10:1270–1279.
Sanes JR, Cheney JM. 1982. Lectin binding reveals a synapse-specific carbohydrate in skeletal muscle. Nature 300:646–647.
Sanes JR, Lichtman JW. 1999. Development of the vertebrate neuromuscular junction. Annu Rev Neurosci 22:389–442.
Selleck SB. 2000. Proteoglycans and pattern formation. Sugar biochemistry meets developmental genetics. Trends Genet 16:206.
Sogos V, Balaci L, Ennas MG, Dell'Era P, Presta M, Gremo F. 1998. Developmentally regulated expression and localization of fibroblast growth factor receptors in the human muscle. Dev Dyn 211:362–373.
Theiler K. 1989. The house mouse. Atlas of embryonic development. New York: Springer-Verlag. 178 p.
Tumova S, Woods A, Couchman JR. 2000. Heparan sulfate proteoglycans on the cell surface: versatile coordinators of cellular functions. Int J Biochem Cell Biol 32:269–288.
Turnbull J, Powell A, Guimond S. 2001. Heparan sulfate: decoding a dynamic multifunctional cell regulator. Trends Cell Biol 11:75–82.
Velleman SG, Liu X, Eggen KH, Nestor KE. 1999. Developmental regulation of proteoglycan synthesis and decorin expression during turkey embryonic skeletal muscle formation. Poult Sci 78:1619–1626.
von Bernhardi R, Inestrosa NC. 1990. Dermatan sulfate and desulfated heparin solubilized collagen-tailed acetylcholinesterase from the rat neuromuscular junction. Brain Res 529:91–95.